14th Australasian Fluid Mechanics Conference
Adelaide University, Adelaide, Australia
10-14 December 2001

Weakly Turbulent Pipe Flow of a Power Law Fluid

M. Rudman, H. M. Blackburn, L. J. Graham and L. Pullum

Thermal and Fluid Engineering
CSIRO BCE, Graham Rd, Highett, Victoria 3091, AUSTRALIA

Abstract

Experiment and simulation of the weakly turbulent flow of a power law fluid in a pipe are presented. The simulation results under-predict the superficial flow velocity by approximately 30% and there are qualitative differences in the two sets of velocity profiles. Careful examination of experimental and numerical methods and results suggests that the cause of the discrepancy is a more complex rheology than power law in the experimental fluid. The numerical results agree well with previously published work and suggest that the simulation technique is correctly predicting turbulence in a power law fluid.

Introduction

The flow of non-Newtonian fluids in pipes occurs in a wide range of practical applications in the process industries. If the fluid has a significant yield stress, or if its effective viscosity is high, industrially relevant flow rates may occur in the laminar flow regime. However in many cases the flow is turbulent and indeed, there are advantages to operating pipe flows in a transitional flow regime because the specific energy consumption is lowest there and in solids transport, intermittency may be used to keep particles in suspension without the much higher pressure losses of the fully turbulent regime. Although some experimental work has appeared on the transitional and turbulent flow of non-Newtonian fluids, little fundamental understanding exists. General theories of turbulence are lacking for non-Newtonian fluids, and the development of mathematical and computational models is not well advanced.

Computational modelling of non-Newtonian flows, especially using Direct Numerical Simulation (DNS), shows promise in understanding transition and turbulence in these fluids. There have been some DNS of the turbulent flow of polymer solutions with an aim to understanding the causes of drag reduction (e.g. [1], [3]). In these studies, dilute polymer solutions were considered in which shear thinning behaviour was negligible and elongational effects were taken into account using various methods for the extra elastic stresses. For a wide range of important materials, the non-Newtonian rheology is primarily of a shear-thinning nature and there is very little in the literature on CFD modelling of turbulent shear-thinning non-Newtonian fluids without visco-elasticity.

This paper describes a study undertaken of shear-thinning non-Newtonian fluids whose viscosity η can be described using either the Ostwald-de Waele (power law) model, i.e.

$$\eta = K\dot{\gamma}^{n-1}$$

where $\dot{\gamma}$ is the shear rate, K is the consistency and n is the flow index, or the Cross model

$$\eta = \eta_\infty + (\eta_0 - \eta_\infty)/(1 + K\dot{\gamma}^n)$$

where η_0 and η_∞ are the zero and infinite shear viscosities.

Experimental results show that the transition to turbulence may occur more slowly than in Newtonian fluids and at higher (generalised) Reynolds number.

Experimental Method

The test facility consists of a fully instrumented mixing tank that feeds a special non-magnetic Warman International 4x3 centrifugal slurry pump. This pump feeds a 40m x 100mm-diameter pipe loop that passes through an MRI imaging facility before it returns to the mixing tank. Optical windows are installed at the beginning and near the end of the loop, with the second optical window positioned at a downstream end of the loop's straight sections to ensure that established flow conditions are examined. The rig is fully equipped with pressure and bulk flow transducers and is operated under computer control via a Labview SCADA system. A two colour TSI laser Doppler velocimeter (LDV) mounted on an industrial robot is used to measure the axial velocity profiles across the horizontal and vertical diameter of the pipe in the second optical window. Further details of this pipe test loop and associated instrumentation are given [8].

The fluid used in the present investigation was a 0.5 wt% aqueous solution of sodium carboxymethylcellulose (7HF Aqualon CMC supplied by A.C Hatrick). The CMC has a molecular weight of approximately 700 000 and is often modelled as a power law fluid. The rheological parameters of the CMC were obtained using a Bohlin CVO50 constant stress rheometer as well as from analysis of the pressure drop versus bulk flow rate curve in the laminar flow regime in the pipe loop. Curve fits to the data yielded a range of parameters depending upon relatively subtle changes in temperature or shear history. Rheological parameters based on the pipe data were used in the simulations.

	K	n
Bohlin	0.717	0.613
Pipe loop	0.506	0.686

Table 1: Power law rheology parameters for 0.5 wt% CMC solution.

Numerical Method

The spatial discretisation employs a spectral element/Fourier formulation, which allows arbitrary geometry in the (x,y) plane, but requires periodicity in the z (out-of-plane) direction. The non-linear terms of the momentum equation are implemented in skew-symmetric form because this has been found to reduce aliasing errors. To allow a semi-implicit treatment of the viscous terms, the non-Newtonian viscosity is decomposed into a spatially-constant component, η_R, and a spatially-varying component η-η_R. The spatially varying component is treated with a second-order explicit formulation and the constant component is treated implicitly, thus enhancing the overall numerical stability of the scheme (see [6] for details). The value of η_R is chosen to be approximately equal to the maximum value of η. This value is not known *a priori*, but can be adjusted during the computation without any adverse effects.

In order to drive the flow in the axial (z) direction, a body force equal to the pressure gradient measured in the experiments is applied to the z-momentum equation. This approach allows the pressure to be periodic in the axial direction.

The code runs in parallel using the message-passing kernel MPI, and the computations reported here were carried out using 8 processors on an NEC-SX5 supercomputer.

Validation

The underlying numerical code has been validated for both DNS and LES of pipe and channel flow (see for example [9]). The implementation of the power-law non-Newtonian viscosity was validated against laminar pipe flow and axisymmetric Taylor-Couette flow of power-law fluids, both of which have analytic solutions. In all cases, numerical results from the code agreed to within 0.01% of theory.

Computational Parameters

The computational domain consists of 105 8th–order elements in the pipe cross section (see Figure 1) and 96 Fourier modes in the axial direction (3πD long). Numerical integration was continued until such time as the solution had become statistically steady. Averages were then taken over approximately 5 pipe-length traverse times. In terms of wall units, the near-wall mesh spacing is $r^+\approx 0.5$, $R\theta^+\approx 8$ and $z^+\approx 35$. This resolution is marginal in the stream-wise direction but sufficient for this initial investigation.

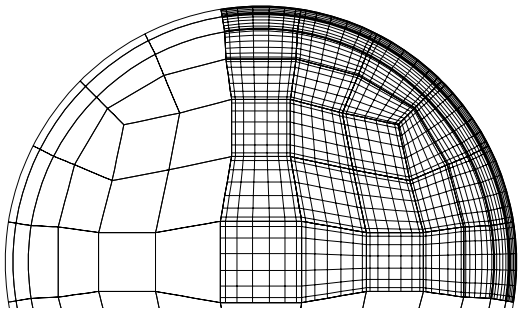

Figure 1 Upper part of the 2-D cross-sectional mesh used for the DNS (the nodal mesh is shown on the right side only). A Fourier expansion with 96 modes was used in the axial direction.

Results

Experimental Results

The transport characteristics of the CMC were measured (i.e. pressure drop as a function of superficial velocity) and it was observed that transition from laminar to turbulent flow was delayed and occurred at a generalised Reynolds number of approximately 3,500 (as opposed to approximately 2,300 as previously reported for both Newtonian and power law fluids). The generalised Reynolds number is based on a wall viscosity that is determined from the mean wall shear stress. The wall shear stress is found from

$$\tau_w = \frac{D}{4}\frac{\partial P}{\partial z}.$$

Assuming a power-law rheology, it is then easy to show that

$$\eta_w = K^{1/n}\tau_w^{1-1/n}, \qquad (1)$$

and this value is then used along with the bulk (or superficial) flow velocity and pipe diameter to define Re_G. This Reynolds number is different to the conventional *K'* and *n'* terms of the Metzner Reed approach.

The mean axial velocity profile for the CMC as measured by LDV is presented in Figure 2. For comparison, the DNS profile for a Newtonian flow at Re=5,000 are included. From this data, it is difficult to distinguish between the CMC and Newtonian results. Further consideration of the experimental results will be included in a discussion of the numerical results.

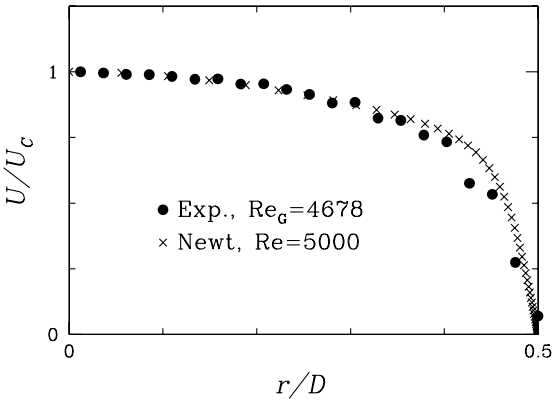

Figure 2 Experimentally measured velocity profiles for CMC compared to DNS results for a Newtonian fluid at Re=5,000.

Numerical Results

The results from three simulations are presented here. In Simulation 1, a pressure gradient equal to that measured experimentally is used (resulting in Re_G=3964). When the pressure gradient used in the simulation is equivalent to that measured experimentally, a mean flow velocity of 0.73 times that of the experiment is predicted. In Simulation 2, an increased pressure gradient (25% above the experimental value) is applied (giving Re_G=5500). The mean flow velocity increases, but only to 0.89 times the experimental value. Both simulation 1 and 2 use the power law rheology model. In simulation 3, the Cross model was used with a higher pressure gradient than experiment (resulting in Re_G=4723) and a similar mean flow velocity as simulation 2. Further consideration of the discrepancy is presented later.

The wall streaks for all simulations show significant axial extent (Figure 3) especially for Simulation 1. The small disordered patches of red (most prevalent in Simulation 2 Re_G=5500) are suggestive of intermittency or bursting, and not of fully developed turbulence.

Velocity profiles in wall units are presented in Figure 4 for the experimental results, the three non-Newtonian CFD simulations and a DNS of turbulent pipe flow at Re=5000. The non-dimensionalisation is undertaken using the wall viscosity given in equation 1. The Newtonian profile is in good agreement with accepted profile for low-Reynolds number turbulent pipe flow (shown as the solid line). All profiles have a linear relationship between U^+ and y^+ in the near wall region. In the logarithmic region (where the flow is represented by $U^+ = A + B\ln y^+$), the experimentally measured profile for the CMC is very much above the low-Re Newtonian profile and has generally similar characteristics to a flow that is not fully developed. The profiles are consistent with results presented in [5] in which the offset *A* increases with CMC concentration (i.e. decreasing *n*) and the results of [7] where *B* increases with increasing CMC concentration as does the buffer layer thickness.

The results for Simulation 1 (Re_G=3964) fall above the low-Re Newtonian profile but significantly below the experimentally measured profile. The results for Simulation 2 lie still closer to the Newtonian profile. As Re_G increases, the simulation results appear to approach the Newtonian profile, consistent with more developed turbulence as Re_G increases, but in disagreement with the experimental data measured here as well as that presented in [5] and [7] for CMC.

A number of different causes for this discrepancy have been investigated but none satisfactorily explain the difference. They include the following:

1. Inconsistencies between the LDV data and the magnetic flow meter were observed that account for approximately 4 of the 25% error in the Re_G=3964 simulation.

2. As seen in Figure 3, the near wall structures have lengths that are comparable to the domain length (especially for Simulation 1 at Re=3964). This will influence the results, although a similar simulation undertaken on a short domain of length πD resulted in an almost identical under-prediction of the mean velocity. Although domain length is an issue, it is not likely to be a major source of the error in mean flow velocity or profiles.
3. Because the power law model for the CMC solution had been determined from shear rates less than approximately 500 sec^{-1}, and the peak values in the turbulent boundary layer where predicted to be of the order of 5000 sec^{-1}, the suitability of both the power law model parameters and the power law itself were called into question. In particular, the possibility of a high shear rate viscosity plateau (more appropriately modelled using a Cross viscosity model) modifying the turbulent structures was a possibility. Even though Cross model parameter fitting from rheology data suggested that the high shear plateau occurs for this material at significantly higher shear rates than those predicted here, Simulation 3 was undertaken using the Cross model (Re_G=4723). Results are seen to be consistent with the power law results (see Figure 3–Figure 6) and is not a source of error.

It was estimated that the highest shear rates in the turbulent boundary layer had time scales that were approximately two orders of magnitude too long for viscoelastic effects to be important. However rheology measurements and turbulent pipe flow measurements of CMC solutions presented in [5] suggest that first normal stress differences in CMC solutions are significant at concentrations higher than 0.2% and result in drag reduction. This is consistent with the discrepancy between experiment and CFD here and it is believed that the discrepancy between experiment and CFD is due to CMC rheology that is not well modelled as a simple power law fluid once the flow becomes turbulent.

Results presented in [2] support this claim. For the turbulent flow of Carbopol 934 (claimed to be well modelled with a power law rheology) over a range of concentrations and flow rates, the logarithmic velocity profile is shown in [2] to be a function of the power law index, n:

$$U^* = \frac{3.8}{n} + \frac{2.78}{n}\ln y^*, \quad \text{where} \quad y^* = \left(\sqrt{\rho^n \tau_W^{2-n}}\Big/K\right) y \,. \quad (2)$$

This correlation is plotted along side the simulation and CMC data in Figure 5. As shown, the results for the CMC experiment deviate significantly from Equation 2, but the CFD results are in extremely good agreement and approach the experimental correlation as Re_G increases. Additional support for the veracity of the simulation results is found in the results of [4] for turbulent flow of a well-sheared Laponite suspension (a synthetic clay that produces a thixotropic fluid). In [4] the profile for transitional flow appears very much like the experimental profile measured here for CMC, however as Re_G increases, the value of A falls from around 8 and approaches the Newtonian value (albeit at much higher Reynolds numbers than simulated here). The value of B does not vary significantly from the Newtonian value once the flow becomes fully developed. On this basis, the simulation results here are believed to give a good representation on the behaviour of weakly turbulent power law fluids.

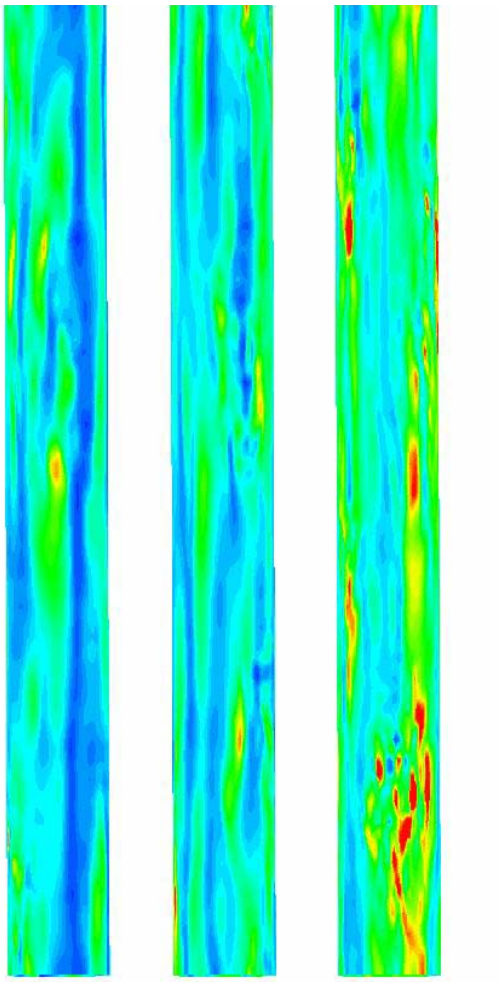

Figure 3 Near wall structure revealed in contours of streamwise velocity at y^+=10. From left to right: Simulation 1, (Re=3964), Simulation 3 (Re_G=4723) and Simulation 2 (Re_G=5500).

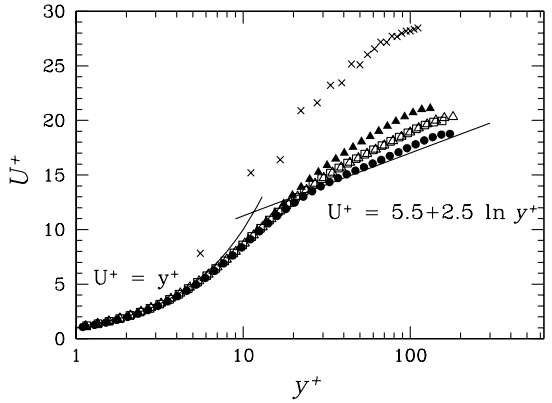

Figure 4 Velocity profiles in wall units: × Experiment (Re_G=4678), ▲ Simulation 1 (Re_G=3964), ❑ Simulation 3 (Re_G=4723), △ Simulation 2 (Re_G=5500) and ● Newtonian (Re=5000).

Turbulence intensities and Reynolds stresses are presented in Figure 6. From the experimental results, only azimuthal and axial turbulence intensities are available. The radial and azimuthal turbulence intensities are lower by 20-40% for the power law fluid simulations compared to the Newtonian DNS, whereas the axial intensities are marginally higher. Interestingly, the CFD results for Re_G=3964 are quite close to the experimental results measured here despite the other discrepancies.

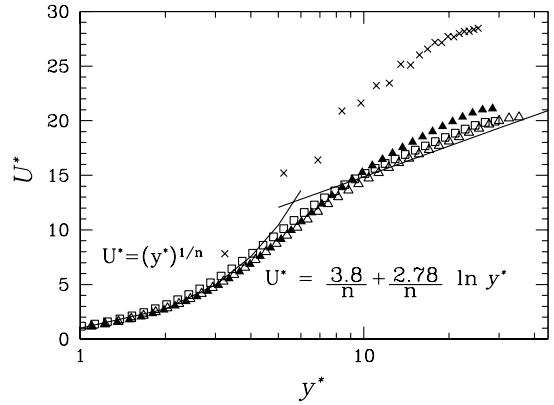

Figure 5 Velocity profiles in wall units: ✕ Experiment (Re_G=4678), ▲ Simulation 1 (Re_G=3964), ❑ Simulation 3 (Re_G=4723) and △ Simulation 2 (Re_G=5500)

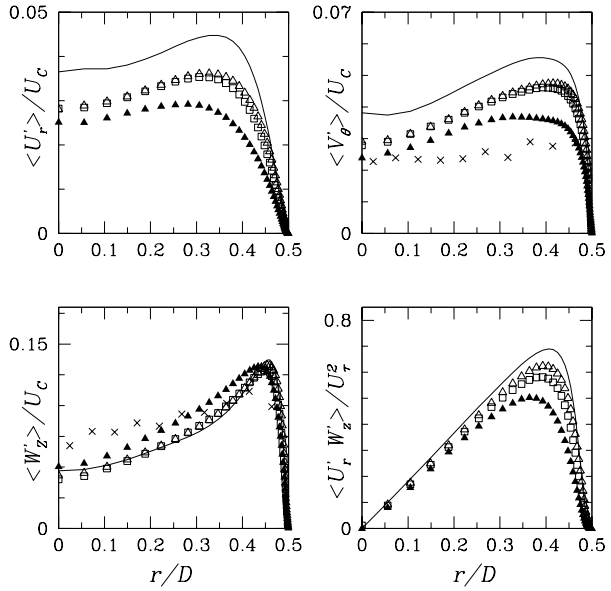

Figure 6 Turbulence intensities and Reynolds stress as a function of *r/D*. Radial velocity (top left), azimuthal velocity (top right), axial velocity (lower left) and Reynolds stress (lower right). Solid line for Newtonian DNS, symbols as for Figure 5.

Cross-sectional velocities for Re_G=5500 are shown in Figure 7 and show a qualitatively similar picture to low Reynolds number turbulence in a Newtonian fluid.

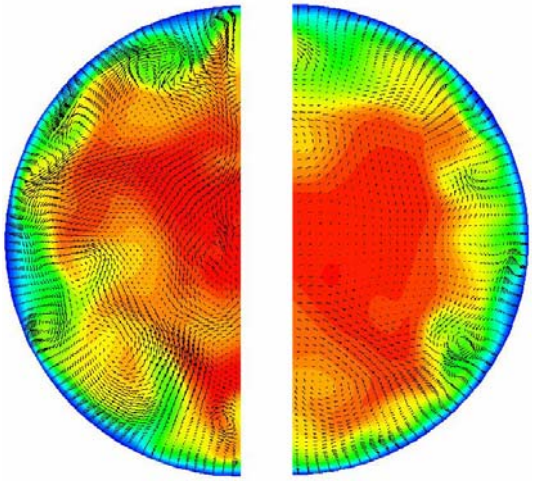

Figure 7 Contours of axial velocity (red is high, blue low) and in-plane velocity vectors for Newtonian flow at Re=5000 (left) and power law fluid at Re_G=5500 (right).

Discussion

The experimental measurements reported here are in qualitative and quantitative agreement with previously published experimental results for CMC [5], [7] and are believed to be correct. They also share some features of transitional flow in shear thinning thixotropic fluids [4], however differ qualitatively from experimental results for power fluids reported in [2]. The simulation results for a power law fluid show some agreement as well as some significant differences with the experimental results. Importantly, the superficial velocity and velocity profiles for a given pressure drop differ significantly. The results are consistent with turbulence suppression, drag reduction and delayed transition in the experiment. These observations, coupled with the inability to match the DNS results to the experiment or data previously reported in [5] all point to a 0.5% CMC solution having more complex rheological properties than a simple power law fluid. Despite this, it is certainly true that CMC is generally well described by this model in the macro sense and that the laminar flow profiles measured in the pipe were in good agreement with power law predictions.

The simulation results have a different form to the experimental results for CMC (Figure 4, Figure 5). The mean flow profiles have some qualitative agreement with experimental results for the shear thinning turbulent flow of Laponite [4], although this is probably fortuitous given that shear history effects that are not included in the DNS are important in Laponite. Importantly, the DNS results are in good agreement with the experimental data of [2] for a power law fluid, with results close to the log law profile measured experimentally there. Additional simulations for different power law indices (n) and higher Re_G need to be undertaken to confirm this result, although it is believed the simulations are correctly predicting turbulence of a power law fluid.

Acknowledgments

The authors acknowledge the support (via AMIRA project P599) of AMIRA, BHP, De Beers, Rio Tinto, Western Mining Corporation and Warman International in sponsoring part of the work described in this paper.

References

[1] Beris, A. N. and Dimitropoulos, C. D.. Psuedospectral simulation of turbulent viscoelastic channel flow, *Comput. Methods Appl. Mech. Engrg,* **180,** 365-392, 1999.

[2] Clapp, R. M. (1961). Turbulent heat transfer in pseudoplastic non-Newtonian fluids. *Int. Dev. Heat Transfer* part III, New York.

[3] Dimitropoulos, C. D.,Sureshkumar, R. and Beris, A. N.. Direct numerical simulation of viscoelastic turbulent channel flow exhibiting drag reduction: effect of the variation of rheological parameters, *J. Non-Newtonian, Fluid Mech.,* **79,** 433-468, 1998.

[4] Escudier, M.P. and Presti, F. Pipe flow of a thixotropic liquid, *J. Non-Newtonian Fluid. Mech.* **62** 291-306, 1996.

[5] Escudier, M.P., Presti, F. and Smith, S. Drag reduction in the turbulent pipe flow of polymers, *J. Non-Newtonian Fluid. Mech.* **81** 197-213, 1999.

[6] Karniadakis, G.E., Israeli, M. and Orszag, S.A. High-Order Splitting Methods for the Incompressible Navier-Stokes Equations, *J. Comput Phys.* **97** 414-443 1991.

[7] Pinho, F.T. and and Whitelaw, J.H., Flow of non-Newtonian fluids in a pipe, *J. Non-Newtonian Fluid. Mech.* **34** 129-144, 1990.

[8] Pullum, L. and L.J.W. Graham, A new high concentration pipeline test loop facility. in *Hydrotransport 14*. Maastrict, Netherlands 1999.

[9] Rudman, M. and Blackburn, H.M., 'Large eddy simulation of turbulent pipe flow', 2nd International Conference on CFD in the Minerals and Process Industries, Melbourne Australia, 6-8 December 1999.